

HTS Josephson junction cantilever microscopy of microwave devices

Felix Stewing, Christian Brendel, and Meinhard Schilling

Abstract—Josephson junctions from the high-temperature superconductor $\text{YBa}_2\text{Cu}_3\text{O}_7$ are routinely used on a cantilever to detect spatially resolved microwave emission from room temperature microwave devices. The Josephson junctions are operated in a temperature range between 40 K to 80 K cooled by a cryo-cooler. Near field imaging is accomplished with operating distances of the cooled Josephson cantilever to the surface of the device under test down to 15 μm . Due to the realization as an active cantilever, a topographic image of the device under test as well as the microwave power distribution can be obtained. We discuss measurements of the three-dimensional radiation distribution above the chip surface under investigation at frequencies ranging from 14 to 762 GHz. We demonstrate characterization of passive microwave devices by measurements of an edge coupled filter, a branch-line coupler and an oversized waveguide.

Index Terms—Josephson junctions, Josephson radiation detectors, Microscopy, Microwave circuits

I. INTRODUCTION

THE operation frequency of integrated microwave devices steadily increases. Analysis of the microwave properties can be accomplished by classical means of network analyzers and specialized probe heads up to 325 GHz [1]. Record values of oscillator circuits based on single transistors in SiGe-technology already reach 400 GHz [2]. In superconducting circuits a RSFQ-frequency divider in Nb-technology operating up to 750 GHz has been demonstrated [3]. The analysis of circuits at these very high frequencies requires new measurement methods and instruments [4]. Signals with frequencies up to several THz can be detected by Josephson junctions from high temperature superconductors [5,6]. With the Josephson cantilever we recently demonstrated an approach where micrometer spatial resolution can be combined with high spectral and power resolution in broadband analysis up to frequencies of the THz-regime [7,8].

To characterize microwave devices operating at room temperature, the cooled cantilever approaches the surface of the device under test without any window inside a vacuum chamber with minimum distance of about 15 μm .

Manuscript received 14 August 2008. We wish to acknowledge the financial support of C. Brendel by the Braunschweig International Graduate School of Metrology.

M. Schilling, C. Brendel, and F. Stewing are with the Institut für Elektrische Messtechnik und Grundlagen der Elektrotechnik, Technische Universität Braunschweig, Germany. (corresponding author: M. Schilling, +49-531-391-3866; fax: +49-531-391-5768; e-mail: m.schilling@tu-bs.de).

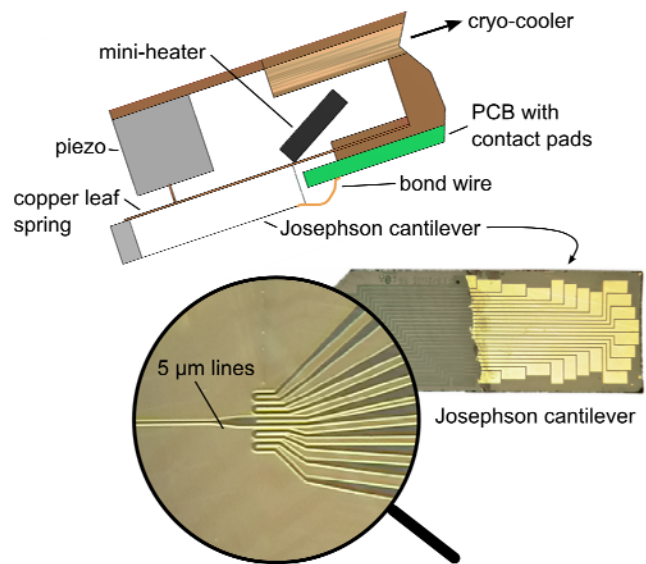


Fig. 1. Schematic drawing of the Josephson cantilever head in the microscopy set-up. The magnification inset shows the 5 μm wide Josephson junctions.

The electromagnetic field couples to the Josephson junction and the resulting suppression of the critical current or the change in differential resistance due to Shapiro steps can be used to determine the detected microwave power and to depict it two-dimensionally. Within the dynamic range applied here the suppression of the critical current is a linear measure of the induced microwave power [8].

For short, for the Josephson cantilever a $\text{YBa}_2\text{Cu}_3\text{O}_7$ film has been deposited by KrF-excimer laser deposition on a 1 mm thick 24° symmetric LaAlO_3 square bicrystal of 10 mm side length. Details of the preparation process have been published earlier [9]. The $\text{YBa}_2\text{Cu}_3\text{O}_7$ film of 130 nm thickness was patterned by photolithography and subsequent argon ion etching into 56 Josephson junctions on 12 cantilevers, which were separated afterwards. The micrograph of one cantilever is magnified in the inset of Fig. 1. The Josephson junctions have a width of 5 μm . The cantilever chip has a width of about 1 mm with a length of 5 mm.

This Josephson cantilever is mounted on a table movable in x- and y-direction with submicrometer resolution [7]. Vertical motion is achieved by combining a third table with oscillatory motion by piezo-driven actor. Contact detection is achieved

via change of resonance frequency of about 40 kHz of the piezo driven copper-leaf spring support of the Josephson cantilever, as depicted in Fig. 1. To cool the cantilever it is attached to the copper-leaf spring from which heat is drained by a closed circle cryo-cooler (Leybold Coolpak 6000 / Coolpower 5/100). The end temperature is controlled at the cantilever holder by a calibrated silicon diode-thermometer in close vicinity of the cantilever. The Josephson junctions integrated on this cantilever show at a operation temperature of 56 K a critical current of $I_c = 267 \mu\text{A}$ with a normal state resistance $R_n = 1.13 \Omega$ resulting in a characteristic $I_c R_n$ -product of $302 \mu\text{V}$. For the last measurements discussed in section III, we employed a different Josephson cantilever with a critical current of $I_c = 250 \mu\text{A}$ with $R_n = 1.9 \Omega$ resulting in a characteristic $I_c R_n$ -product of $475 \mu\text{V}$ at operation temperature of 54 K.

II. EDGE COUPLED FILTER

As a first approach, an edge coupled filter of third order has been prepared and measured. It has been designed with Ansoft Designer SV. We obtained in the prepared device a passband frequency of 15 GHz with a passband width of 1.0 GHz. As substrate material we employed aluminum PCB with a dielectric coating of $150 \mu\text{m}$ ($\epsilon_r=4.4$, $\tan\delta = 0.02$ measured at 10 GHz) and $35 \mu\text{m}$ copper plating. The resonators have a width of $100 \mu\text{m}$ and a length of $3000 \mu\text{m}$ with wide gaps of $263 \mu\text{m}$ in the middle and narrow gaps of $175 \mu\text{m}$ at the ends. Fig. 2(a) shows the geometric layout of the investigated filter with a total length of 12 mm. The physical realization of the filter somewhat differs from the design values because of limited manufacturing capabilities. Therefore, for simulation actual geometry values were extracted from optical micrographs. In Fig. 2 (b) the simulated transmission characteristics is shown together with the measured one by conventional network analysis.

The microwave distribution above this filter has been imaged as depicted in Fig. 2(c), which shows a comparison of simulated and measured microwave power distributions. The microwave power distribution above the filter surface at a height of $50 \mu\text{m}$ has been imaged at 4 different frequencies of 15.5, 16, 17 and 18 GHz as given in Fig. 2(c). The images have been recorded point by point with the Josephson cantilever. In each point its complete I-V characteristics have been measured and the values of the critical current have been extracted as a measure of the locally detected microwave power. The output power of the microwave generator has been set to -20 dBm for all measurements. Since the transmission characteristics S_{21} is linear in microwave power, cable and plug frequency dependencies have not been deembedded. Clearly it can be seen in Fig. 2(c), how the decreasing transmittance towards higher frequencies beyond the passband (15.5, 16, 17, 18 GHz) leads to a reduced microwave power level in the first, second and third resonator stage, while the stripline directly coupled to the input displays a rather homogeneous microwave power distribution even at 18 GHz due to reflections. The simulated distributions show minor differences, which have not been understood so far.

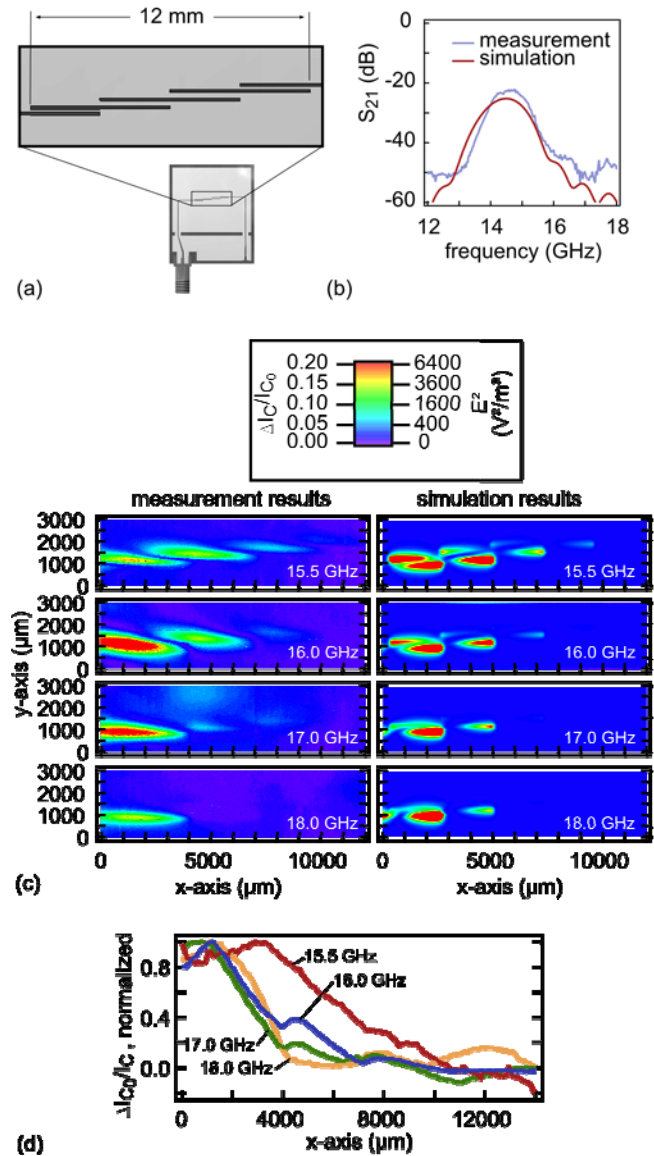


Fig. 2. (a) Layout of the edge coupled filter, (b) simulated and measured transmission characteristics S_{21} , (c) images of the power distribution at 15.5, 16, 17, and 18 GHz, (d) evaluation of the decreasing transmission from resonator to resonator stage within the filter for the different frequencies.

The measured power distribution has been integrated on each vertical scan line across all resonator stages, normalized to the maximum observed value and is depicted along the filter structure in Fig. 2 (d). At 18 GHz, this spatially averaged microwave power level reaches the noise floor already at $4000 \mu\text{m}$ measured from the input port, while at 15.5 GHz the noise floor begins at about $11000 \mu\text{m}$, due to the higher transmittance of the filter at 15.5 GHz.

A reasonable correspondence of simulations and measurements for this device has been found, demonstrating how microwave filter structures can be analyzed in detail with a Josephson cantilever without changing the filter geometry, i.e., for additional output ports, as required for application of conventional network analyzers. While only input and output ports are accessible with a network analyzer, our method can access arbitrary points of a circuit and no physical

modifications (plugs etc.) are necessary. These contactless measurements can open new insight into the properties of microwave filters.

III. DIRECTIONAL COUPLER

The directional coupler is another very important passive microwave device, which has been investigated with the Josephson cantilever. It serves to distribute microwave power from the input lines to all output lines according to well defined ratios. With outer dimensions of $2.5 \times 2.9 \text{ mm}^2$ on the same aluminum PCB as for the edge coupled filter in section II, the line width of the copper lines has been chosen as $200 \mu\text{m}$ for narrow and $400 \mu\text{m}$ for wide lines. The layout of the branch-line coupler is depicted in Fig. 3(a).

The ideal branch-line coupler at its design frequency would have no microwave power distributed to port P_4 while the power from port P_1 divides equally to port P_2 and P_3 . The use of stubs leads to imperfect dump impedances and to standing waves in the circuit. In Fig. 3(b) the transfer characteristics from port P_1 to the output ports $P_2 - P_4$ are shown, as simulated for the actual measured coupler dimensions. The high losses of the substrate material together with the imperfect dump impedances lead to a non-ideal coupler performance.

The spatially dependent microwave distribution has been measured by the Josephson cantilever and is depicted for 18 GHz (see Fig. 3(c)). Nevertheless, our measurements give interesting insight into the structure. We find a standing wave at the input line with relatively high microwave power. Above the lines to output port P_2 and P_3 one can see almost equal power levels while above the line to port P_4 only very little power emission is observed, as expected for the branch-line coupler. Beside the expected microwave distribution along the lines of the branch-line coupler further hot spots are detected, which are most probably due to imperfections in the manufactured structures.

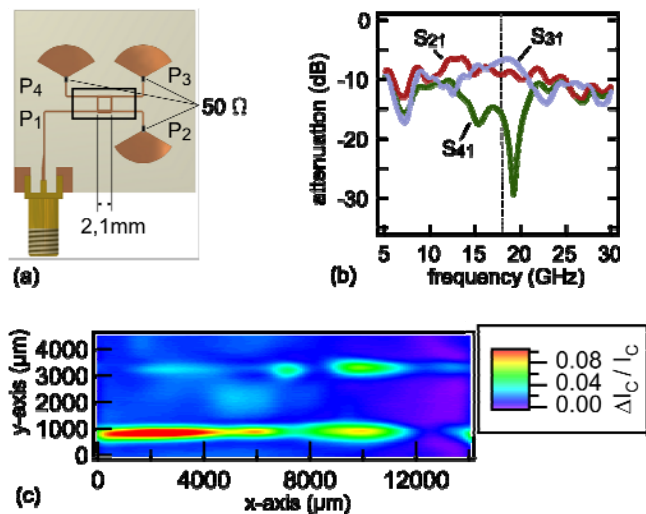


Fig. 3. (a) Layout of a branch-line coupler for 20 GHz, (b) calculated transfer characteristics, (c) planar microwave power distribution of the branch-line coupler imaged within the black box marked in (a).

IV. WAVEGUIDE

As an example for the high frequency capabilities and the three-dimensional imaging possibilities, the power distribution at the end of an oversized multimode circular waveguide for far-infrared radiation at 762 GHz has been investigated in order to analyze the spatial mode distribution. The waveguide is fed by far-infrared light from a molecular laser with about 2 mW output power pumped by a CO₂-laser system Edinburgh Instruments PL3 with about 7 W output power. From the output of the far-infrared laser to the scanning microscope based on the Josephson cantilever, the light wave is guided by a oversized brass waveguide of 6 mm diameter and a length of 120 cm. The far-infrared radiation is coupled to the vacuum chamber of the microscope by waveguide fed-through into the waveguide under investigation. From the Gaussian power distribution of the laser beam in free air the radiation excites more than 100 modes in the oversized waveguide. For the measurements shown below a dielectrically filled tapered waveguide with 3 mm diameter at its open end has been excited to achieve a field concentration in the middle of the waveguide as shown in Fig. 4(a). The I-V curve and its corresponding differential resistance under illumination with the radiation of 762 GHz are depicted in Fig. 4(b). The response of the Josephson junctions to the 762 GHz radiation can be clearly seen in the differential resistance.

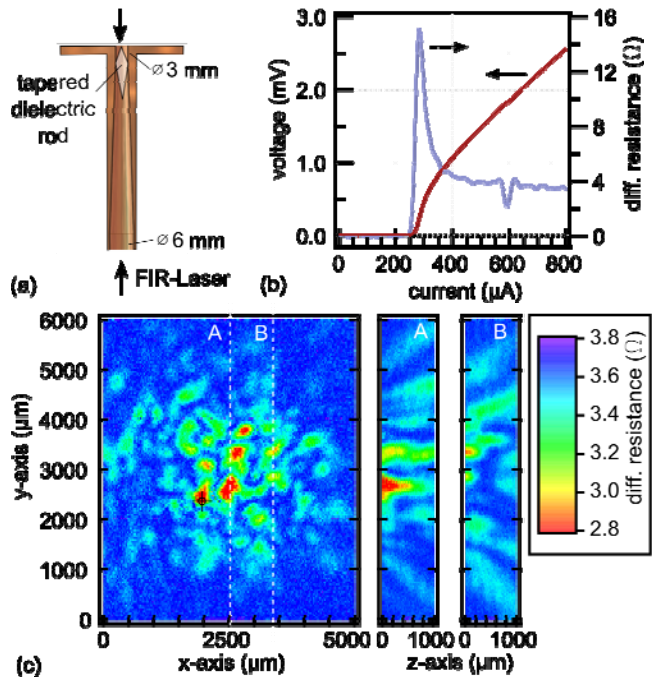


Fig. 4. (a) Geometry for the characterization of the waveguide, (b) I-V curve and differential resistance of the employed Josephson cantilever, (c) corresponding measured microwave power distribution in three dimensions.

As depicted in Fig. 4(c), the Josephson cantilever can be used to determine the three dimensional radiation pattern above the open end of the tapered waveguide. In the pattern scanned in the z-axis direction along the oversized waveguide clearly a radiation cone angle of 45 degree by diffraction at the edges of the waveguide is resolved. In Fig. 4(c) also the obtained image perpendicular to the open waveguide end is shown. As

expected, we reproducibly find a multimodal radiation distribution.

V. CONCLUSION

In conclusion, we prepared an edge coupled filter and a branch-line coupler and characterized these structures by their frequency dependent spatial microwave power distribution. We demonstrate how transmission values can be obtained this way, opening the route to local network analysis in circuits. We further demonstrate the high frequency capabilities of the scanning microwave microscope based on the Josephson cantilever by imaging three dimensional microwave distribution at the open end of a multimode circular waveguide at 762 GHz.

REFERENCES

- [1] Oleson Microwave Labs, www.oml-mmw.com
- [2] R. Krithivasan, Y. Lu, J. D. Cressler, J.-S. Rieh, M. H. Khater, D. Ahlgren, and G. Freeman, *IEEE Electron Device Lett.* **27**, 567 (2006).
- [3] W. Chen, A.V. Rylyakov, V. Patel, J.E. Lukens, and K.K. Likharev, *Appl. Phys. Lett.* **73**, 2871 (1998).
- [4] B. Rosner and D.W. van der Weide, *Rev. Sci. Instrum.* **73**, 2505 (2002).
- [5] Y.Y. Divin, H. Schulz, U. Poppe, N.Klein and K. Urban, V.V. Pavlovskii, *Appl. Phys. Lett.* **68**, 1561 (1996).
- [6] A. Kaestner, M. Volk, F. Ludwig, M. Schilling, and J. Menzel, *Appl. Phys. Lett.* **77**, 3057 - 3059 (2000).
- [7] M. Schilling, A. Kaestner, and F. Stewing, *Appl. Phys. Lett.* **88**, 252507 (2006).
- [8] F. Stewing, C. Brendel, and M. Schilling, *Frequenz* **77**, 3057 (2000).
- [9] J.-K. Heinsohn, D. Reimer, A. Richter, K.-O. Subke, and M. Schilling, *Physica C* **299**, 99 (1998).